

## Comparison hybrid techniques-based mixed transform using compression and quality metrics

Zainab Ibrahim Abood Al-Rifae<sup>1</sup>, Samir Ibrahim Abood<sup>2</sup>, Tarik Zeyad Ismaeel<sup>1</sup>

<sup>1</sup>Department of Electrical Engineering, College of Engineering, University of Baghdad, Baghdad, Iraq

<sup>2</sup>Department of Electrical and Computer Engineering, Prairie View A&M University, Prairie View, Texas, USA

### Article Info

#### Article history:

Received Oct 9, 2022

Revised Jan 26, 2023

Accepted Jan 29, 2023

#### Keywords:

Comparison

Compression metrics

Discrete wavelet transform

Hybrid techniques

Multi-wavelet transform

Quality metrics

Tensor product mixed transform

### ABSTRACT

Image quality plays a vital role in improving and assessing image compression performance. Image compression represents big image data to a new image with a smaller size suitable for storage and transmission. This paper aims to evaluate the implementation of the hybrid techniques-based tensor product mixed transform. Compression and quality metrics such as compression-ratio (CR), rate-distortion (RD), peak signal-to-noise ratio (PSNR), and Structural Content (SC) are utilized for evaluating the hybrid techniques. Then, a comparison between techniques is achieved according to these metrics to estimate the best technique. The main contribution is to improve the hybrid techniques. The proposed hybrid techniques are consisting of discrete wavelet transform (W), multi-wavelet transform (M), and tensor product mixed transform (T) as 1-level W, M, and T techniques. WT and MT are the 2-level techniques, while WWT, WMT, MWT, and MMT are the 3-level techniques. For each level of each technique, a reconstructed process is applied. The simulation results using MATLAB 2019a indicated that the MMT is the best technique with CR=1024, R(D)=4.154, and PSNR=81.9085. Also, it is faster than the other techniques in the previous works as compared with them. Further research might investigate whether this technique can benefit image and speech recognition.

This is an open access article under the [CC BY-SA](https://creativecommons.org/licenses/by-sa/4.0/) license.



### Corresponding Author:

Zainab Ibrahim Abood Al-Rifae

Department of Electrical Engineering, College of Engineering, University of Baghdad

Baghdad, Iraq

Email: zainab.ibrahim@coeng.uobaghdad.edu.iq

## 1. INTRODUCTION

It is essential and very complex to find orthogonal matrices in various sizes, which can be used in various communication and image processing [1]. The orthogonal matrix as a transform filter is used for mixed transform generated using the tensor product-based data processing. The evaluation and analysis of this mixed technique in the image compression-based discrete wavelet transform mixed and slantlet with the tensor product is presented in [2]. Mohammed *et al.* [1] introduced a method to find an orthogonal matrix by using a tensor product between two orthogonal matrices of imaginary and real numbers with applying it to images and communication signal processing. The output matrix is also orthogonal, and this method's processing is easy compared to the basic proofs used in classical methods. In image compression, Kumar *et al.* [3] used singular value thresholding and truncation to get a low-rank matrix completion for a decomposed image to obtain the low rank of the compressed image. A thresholding algorithm is applied to retrieve the quality of this image. They mentioned that from the results, it is clear that 80% compression is attained with acceptable visual quality as in a human vision system.

Boudida *et al.* [4] introduced textural quality analysis for a compressed image and used the second generation of wavelet transform to enhance the compression process in biometric images. They utilized a quincunx wavelet transform joint to a modified advanced encoder called SPIHT-Z encoding. The compression process's paramount importance is minimizing the bit space requisite to transmit or store information of various types [4], [5]. Hu *et al.* [6] proposed a randomness map to measure the masking effect to capture the features of the human visual system. A pre-processing scheme is used to simulate the occurrences' processing in the initial portion of the human visual system. Wahed *et al.* [7] tested wavelet and multi-wavelet filter banks with images, adding more useful analysis. Filter bank properties such as compact support, orthogonal, phase response, and symmetry are essential parameters that affect the mean square error and professed image quality. The compression of grayscale image performance was compared with an expected scalar wave. Subjective quality measures and a peak signal-to-noise ratio are used to assess the performance.

Aboud [8] presented three techniques: a three-dimension 2-level wavelet transform, a three-dimension 2-level multi-wavelet transform, and a three-dimension 2-level hybrid technique. The last technique combines wavelet and multi-wavelet transform. These techniques are compared to the retained compression ratio, entropy, energy, percent root mean square difference, and peak signal-to-noise ratio. The result is that the best technique for image compression is the three-dimension two-level hybrid technique. A discrete cosine and wavelet transform technique are used for white flower image fusion. Intensity hue saturation, red, green, and blue (RGB) values of fused and individual images are evaluated using peak signal-to-noise ratio (PSNR) [9]. Image quality is objectively and technically described in [10] to indicate a deviation from a reference model, and it is also related to a subjective perception of an image. The characteristic property of the image can be considered as image quality evaluation by which degradation of the perceived images is measured and calculated compared to the reference image. A comparative study on full-reference fusion methods is presented in [11]. It is discovered that the rank aggregation-based full-reference fusion can outperform other full-reference fusion approaches and the top-performing full-reference methods. The mean squared error and signal to noise ratio have been used to measure the image quality.

PhiCong *et al.* [12] presented a novel light field image quality assessment (LF-IQA) metric with low computational complexity to enhance the conventional LF-IQA. Memon *et al.* [13] proposed an image processing approach that collects three image descriptors as a feature extraction phase. Pre-processing techniques of 100 classes of handwritten Arabic databases are used to prepare the testing and training datasets. The best k-nearest neighbor's algorithm is used to classify the Arabic handwritten images [14]. Seetharamaswamy *et al.* [15] proposed dual-dictionary learning as prime and residual-dictionary learning. Reconstructing the central high frequency and high residual frequency is required to recover the finer image details. Saeed *et al.* [16] applied operations such as histogram, conversion into grayscale, erosion, dilation, and close and open operations on four different images. Then it is followed by a retrieving process to the original image. Patel *et al.* [17] focused on a comparative analysis of various image pre-processing techniques executed on flower images. The performance assessment of these techniques depends on their ability to remove noise in the flower images. Root mean square error and peak signal-to-noise ratio methods are used for performance evaluation. Aboud [18] presented three composite techniques-based color image compression to achieve images with good image quality and better performance. The composite wavelet technique, composite stationary-wavelet technique, and composite multi-wavelet technique. The low-low sub-band of the 3<sup>rd</sup>. level in each composite transform is calculated. The best technique is the three-level multi-wavelet transform in the composite multi-wavelet technique. That is because it has the maximal values of energy, compression ratio (CR), and lowest values of the computation time (T) and rate-distortion (RD).

This paper compares hybrid techniques-based tensor product mixed transform using compression and quality metrics. It aims to evaluate the implementation of the hybrid techniques; The main contribution is to improve the hybrid techniques which consists of 1-level (discrete wavelet transform (W), multi-wavelet transform (M), and tensor product mixed transform (T)) techniques, 2-level (WT and MT) techniques, and 3-level (WWT, WMT, MWT, and MMT) techniques. The novelty in this work is that the 3<sup>rd</sup>. level in the hybrid techniques is the tensor product mixed transform which improve the image compression and image quality of the technique and reduce the computation time. Compression and quality metrics will be computed for each final level, and a comparison between techniques will be implemented according to these metrics. The compression metrics are; compression ratio, mean square error, rate distortion, and peak signal-to-noise ratio. At the same time, the quality metrics used are; average difference, maximum difference, normalized absolute error, and structural content.

This paper contains the following sections: In section 2, the research method for the proposed techniques with an explanation of each stage in it, the image quality, and compression metrics used are presented. Section 3 introduced the simulation results and evaluation of the performance of the techniques. Finally, in section 4, the conclusion of this study is explained with some perspective's future works.

**2. RESEARCH METHOD**

**2.1. Overview**

The proposed technique's block diagram is shown in Figure 1. It consists of an image pre-processing stage followed by hybrid techniques those contain three types of transforms; discrete wavelet transform, multi-wavelet transform, and tensor product mixed transform. These techniques are 1-level techniques, 2-level techniques, and 3-level techniques. Then a comparison among these techniques according to the image compression and quality metrics computation will be implemented. Finally, a comparison decision is decided on which technique is the best.

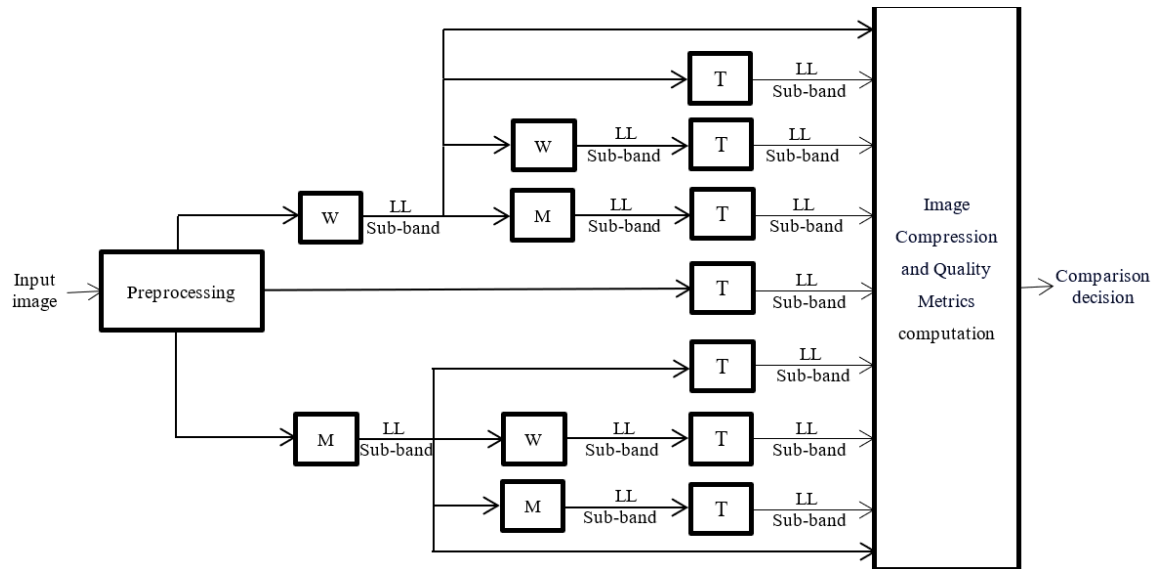


Figure 1. The proposed technique's block diagram

**2.2. Image pre-processing**

Image pre-processing is the primary step for reducing the distortion and noise removal of the original image to enhance its quality [17], [19]. In this paper, the original input image is a gray or color image of any size. If it is a color image, convert it to a gray image to reduce the computation complexity. Finally, the gray image is converted to the double-precision form and resized to the size (1024\*1024) pixels to be a power of 2 and square.

**2.3. The hybrid techniques**

These techniques appear in three different types. Firstly, 1-level techniques contain three 1-level techniques, W, M, and T. Secondly, 2-level techniques contain two 2-level techniques, WT and MT. Finally, 3-level techniques contain four 3-level techniques, WWT, WMT, MWT, and MMT.

**2.3.1. 1-level techniques**

There are three techniques illustrate 1-level techniques, which are W, M, and T:

- W technique: discrete wavelet transforms employ two types of functions, called wavelet functions and scaling functions, which are related to high and low pass filters, respectively [8]. In the first level of decomposition, the image is divided into four sub-bands  $LL_1$ ,  $LH_1$ ,  $HL_1$ , and  $HH_1$ . The LL sub-band has a low-frequency component and can be decomposed into another four sub-bands  $LL_2$ ,  $LH_2$ ,  $HL_2$ , and  $HH_2$  [8], [20], [21]. In the W technique, after the image is processed, a discrete wavelet transform is applied to the processed image as a 1<sup>st</sup> level, so it is (W).
- M technique: multi-wavelet possesses greater than one-scaling function, providing a great degree of freedom and the likelihood of superior performance for the image processing applications compared to a scalar wavelet. The multi-wavelet and multi-scaling functions will satisfy the dilation matrix [8]. The multi-wavelet has two channels, two sets of wavelet coefficients, and two sets of scaling coefficients. Since multiple iterations over a low-pass data are wanted, the wavelet coefficients of the two channels are stored together, and the scaling coefficients of the two channels are also stored together [8], [22], [23]. In the M technique, after the image is processed, a multi-wavelet transform is applied to the processed image as a 1<sup>st</sup> level, so it is (M).

- T technique: tensor product mixed transform is the transfer of the signal or digital image from one domain to another spatial domain using multiple-orthogonal filters transform to collect the properties and benefits of the converters transform in the same signal or image. The T equation is:

$$[T]_{2^i \times 2^i} = [W]_{2^j \times 2^j} \otimes [W]_{2^{i-j} \times 2^{i-j}} \quad (1)$$

where  $j$  is from 1 to  $i-1$ . Then, the matrix relating tensor product is Kronecker multiplied by these two matrices [1], [2], [22], [24]. In T technique, after the image is processed, a tensor product mixed transform is applied to the processed image as a 1<sup>st</sup> level, so it is (T). In this work, the original image size is  $1024 \times 1024$ , i.e.,  $2^{10} \times 2^{10}$ , and tensor product mixed transform is applied to a 2D image, according to (1). A tensor product mixed transform can be created using 2D discrete wavelet transform of different sizes with discrete wavelet transform.

### 2.3.2. 2-level techniques

There are two techniques illustrate 2-level techniques, which are WT and MT:

- WT technique: in the WT technique, after the image is processed, a discrete wavelet transform is applied to the processed image as a 1<sup>st</sup> level. Then a tensor product mixed transform is applied to the low-low sub-band of the discrete wavelet transform as a 2<sup>nd</sup> level, so it is (WT).
- MT technique: in the MT technique, after the image is processed, a multi-wavelet transform is applied to the processed image as a 1<sup>st</sup> level. Then a tensor product mixed transform is applied to the low-low sub-band of the multi-wavelet transform as a 2<sup>nd</sup> level, so it is (MT).

### 2.3.3. 3-level techniques

There are four techniques illustrate 3-level techniques, which are WWT, WMT, MWT, and MMT:

- WWT technique: in WWT technique, a discrete wavelet transform is applied to the processed image as a 1<sup>st</sup> level. Then a discrete wavelet transform is applied to the low-low sub-band of the discrete wavelet transform as a 2<sup>nd</sup> level. Finally, a tensor product mixed transform is applied to the low-low sub-band of the discrete wavelet transform as a 3<sup>rd</sup> level, so it is (WWT).
- WMT technique: in the WMT technique, a discrete wavelet transform is applied to the processed image as a 1<sup>st</sup> level. Then a multi-wavelet transform is applied to the low-low sub-band of the discrete wavelet transform as a 2<sup>nd</sup> level. Finally, a tensor product mixed transform is applied to the low-low sub-band of the multi-wavelet transform as a 3<sup>rd</sup> level, so it is (WMT).
- MWT Technique: in the MWT technique, a multi-wavelet transform is applied to the processed image as a 1<sup>st</sup> level. Then a discrete wavelet transform is applied to the low-low sub-band of the multi-wavelet transform as a 2<sup>nd</sup> level. Finally, a tensor product mixed transform is applied to the low-low sub-band of the wavelet transform as a 3<sup>rd</sup> level, so it is (MWT).
- MMT technique: a multi-wavelet transform is applied to the processed image as a 1<sup>st</sup> level. Then a multi-wavelet transform is applied to the low-low sub-band of the multi-wavelet transform as a 2<sup>nd</sup> level. Finally, a tensor product mixed transform is applied to the low-low sub-band of the multi-wavelet transform as a 3<sup>rd</sup> level, so it is (MMT).

## 2.4. Image compression metrics computation

High-visual quality images with high resolution are getting trendier. Digital images need ample storage space because of their big-data size, which creates an obstacle in transmission and data storage [3], [25]. Also, it needs to keep the quality of a reconstructed image good after its construction, increase the compression ratio [26], and minimize the execution time [27]. Therefore, it is suitable to use image compression that represents the extensive image data into little data using a suitable coding technique [3], [28]. Image compression is the task by which the image is deposited in a compressed form to reduce the size of a stored image to permit better use of the storage space due to the limited storage area [26], [29]-[31]. For the low-low sub-band of the final level in each technique, compression metrics are computed according to (2) to (5).

- Compression-ratio (CR): is the ratio between the size before compression and the size after compression [32], [18], [1]:

$$CR = \frac{\text{Size before compression}}{\text{Size after compression}} \quad (2)$$

So; according to (1) and the compression ratio of each transform in each level, the sizes of the images of the final level in each technique which is; the tensor product mixed transform, are:

$$\begin{aligned}
 [T]_{2^{10} \times 2^{10}} &= [W]_{2^9 \times 2^9} \otimes [W]_{2^1 \times 2^1} \text{ For T Technique} \\
 [T]_{2^{10} \times 2^{10}} &= [W]_{2^8 \times 2^8} \otimes [W]_{2^1 \times 2^1} \text{ For WT Technique} \\
 [T]_{2^{10} \times 2^{10}} &= [W]_{2^7 \times 2^7} \otimes [W]_{2^1 \times 2^1} \text{ For MT Technique} \\
 [T]_{2^{10} \times 2^{10}} &= [W]_{2^6 \times 2^6} \otimes [W]_{2^1 \times 2^1} \text{ For WMT Technique} \\
 [T]_{2^{10} \times 2^{10}} &= [W]_{2^6 \times 2^6} \otimes [W]_{2^1 \times 2^1} \text{ For MWT Technique} \\
 [T]_{2^{10} \times 2^{10}} &= [W]_{2^7 \times 2^7} \otimes [W]_{2^1 \times 2^1} \text{ For WWT Technique} \\
 [T]_{2^{10} \times 2^{10}} &= [W]_{2^5 \times 2^5} \otimes [W]_{2^1 \times 2^1} \text{ For MMT Technique}
 \end{aligned}$$

- Mean square error (MSE): is the mean square of the pixel difference between two images, and it is given by:

$$\text{MSE} = \frac{1}{MN} \sum_{i=1}^M \sum_{j=1}^N (x(i, j) - y(i, j))^2 \tag{3}$$

where  $x(i, j)$  and  $y(i, j)$  represent the original and compressed image. MN is the size of these images [2], [18]. The smaller values of MSE refer to the best results. In this work, the compressed image is the low-low sub-band of the transformed image.

- Rate-distortion (RD): this is the function of the lowest rate that the input signal that can be encoded while keeping a distortion less than or equal to D:

$$R(D) = \frac{1}{2} \log_{10} \left( \frac{\sigma^2}{\text{MSE}} \right) \tag{4}$$

where  $(\sigma^2)$  is the Variance [18].

- Peak signal-to-noise ratio (PSNR): the image quality and similarity between two images can be measured by the PSNR metric. A more significant peak signal-to-noise ratio indicated better image quality and compression [2], [32]:

$$\text{PSNR} = 10 \log_{10} \left( \frac{255^2}{\text{MSE}} \right) \tag{5}$$

**2.5. Image quality metrics computation:**

An important assignment is estimating the image quality for an original or a processed image. There are practical cases when full-reference metrics can be utilized for this purpose, and this takes place when an image is considered a reference image. After processing, one has the processed image that must be compared with the reference using specific quality metrics. Such quality metrics are peak signal-to-noise ratio or mean square error. Alternatively, visual quality metrics (such as structural similarity) both traditional can be applied [12], [33]-[36]. For the low-low sub-band of the final level in each technique, quality metrics are computed according to (6) to (9).

- Average difference (AD): is the pixel difference between two images, and the more significant value of AD refers to the poor quality [36]:

$$\text{AD} = \frac{1}{MN} \sum_{i=1}^M \sum_{j=1}^N (x(i, j) - y(i, j)) \tag{6}$$

- Maximum difference (MD): is the maximum difference between two images and is proportional to the contrast giving a dynamic range of the image. The higher value of the maximum difference refers to the fact that the image has poor quality [37]:

$$\text{MD} = \text{MAX} |x(i, j) - y(i, j)| \tag{7}$$

- Normalized absolute error (NAE): normalizing the absolute pixel difference between two images. The NAE value must be meager to get a good image quality [13]:

$$\text{NAE} = \frac{\sum_{i=1}^M \sum_{j=1}^N |x(i, j) - y(i, j)|}{\sum_{i=1}^M \sum_{j=1}^N x(i, j)} \tag{8}$$

- Structural content (SC): refers to the closeness of two images. The higher structural content value specifies any image's poor quality. For two identical images, the structural content metric is 1(maximum), and the length of the hidden data is zero [37]:

$$SC = \frac{\sum_{i=1}^M \sum_{j=1}^N (y(i,j))^2}{\sum_{i=1}^M \sum_{j=1}^N (x(i,j))^2} \quad (9)$$

## 2.6. Comparison decision

Each metric has a responsibility to play in a controlling of the image compression and quality assessment [37]. After comparing each low-low sub-band of the final level in each technique according to image compression and quality metrics, computation using (2) to (8) has been implemented. A comparison decision is decided on which technique is the best.

## 3. RESULTS AND EVALUATION

Image compression algorithms exploit data redundancies; they identify which data need to be kept to reconstruct the image [8], [15] and which data to be canceled [8]. This paper uses a set of different formats and types of images, and one of them is chosen as a model. Visual results of WWT are assessed for the model image shown in Figure 2. Figures 2(a)-(d) show the pre-processing stage results: the original image, gray image, image after double precision, and resized image.

Figures 2(e)-(l) show the construction and reconstruction of each level in the WWT technique: the (1<sup>st</sup>. level) image after wavelet transform, its reconstructed image, and the LL sub-band image, then (2<sup>nd</sup>. level) image after wavelet transform followed by its reconstructed image, LL sub-band image, finally; the (3<sup>rd</sup>. level) image after tensor product mixed transform, and its reconstructed image. It can be noted that the WWT technique reconstructed image has high image quality.

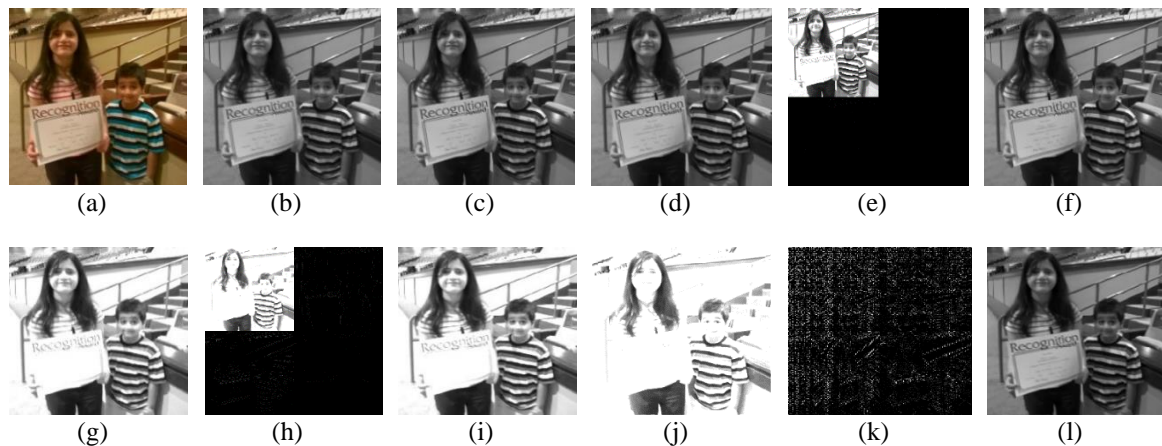


Figure 2. Model of WWT technique (a) original image, (b) gray image, (c) image after double precision, (d) resized image, (e) (1<sup>st</sup>. level) image after wavelet transform, (f) reconstructed image after wavelet transform, (g) LL sub-band image after wavelet transform, (h) (2<sup>nd</sup>. level) image after wavelet transform, (i) reconstructed image after 2<sup>nd</sup>. level wavelet transform, (j) LL sub-band image after 2<sup>nd</sup>. level wavelet transform, (k) (3<sup>rd</sup>. level) image after tensor product mixed transform, and (l) reconstructed image after tensor product mixed transform

Visual results of MMT are assessed for the model image shown in Figure 3. Figures 3(a)-(d) show the pre-processing stage results: the original image, gray image, image after double precision, and resized image. Figures 3(e)-(l) show the construction and reconstruction of each level in the MMT technique, which are; the (1<sup>st</sup>. level) image after the multi-wavelet transform, its reconstructed image, and the LL sub-band image, then (2<sup>nd</sup>. level) image after the multi-wavelet transform followed by its reconstructed image, LL sub-band image, finally; (3<sup>rd</sup>. level) image after tensor product mixed transform, and its reconstructed image.

In the 1<sup>st</sup>. level, the reconstructed image has a size of 1024×1024, and the reconstructed image in the second level has a size of 256×256. Finally, the reconstructed image in the third level has a size of 64×64, and the LL sub-band image after the multi-wavelet transform has the same size. Figures 3(j) and (l) show the LL sub-band image after 2<sup>nd</sup>. multi-wavelet transform and the reconstructed image after tensor product mixed transform have an occurrence of some noise on these images. Indeed, the images do not have any noise, but that is because of the significantly different sizes between the reconstructed images in the three levels. i.e.,



when we collect them in a subplot, the image with the size 64×64 will be changed to the size 1024×1024 so as the image with the size 256×256, when the image is enlarged by a factor of 256, where  $(1024 \times 1024 / (64 \times 64) = 256)$ , the image will get some quality degradation. So, it can be noted that the MMT technique reconstructed image has efficient image compression and image quality.

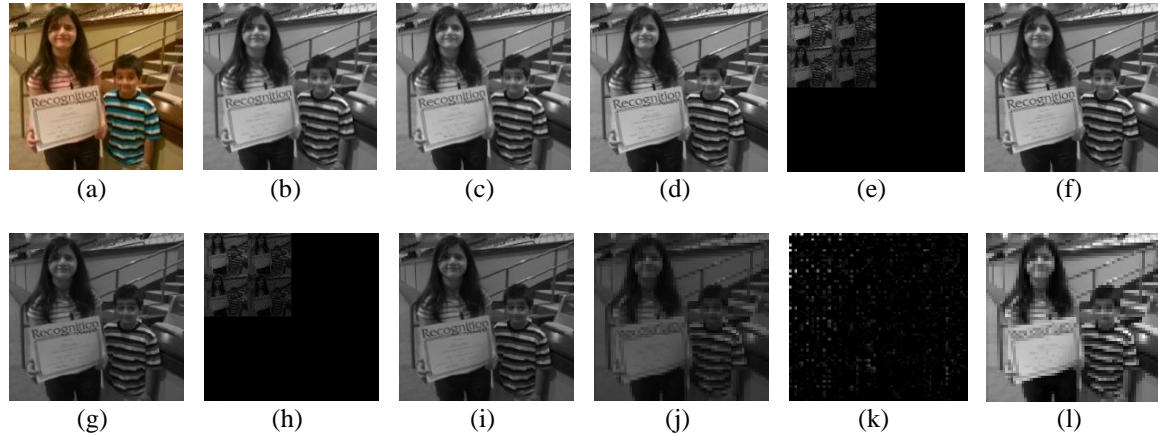


Figure 2. Model of MMT (a) original image, (b) gray image, (c) image after double precision, (d) resized image, (e) (1<sup>st</sup> Level) image after multi-wavelet transform, (f) reconstructed image after multi-wavelet transform, (g) LL sub-band image after multi-wavelet transform, (h) (2<sup>nd</sup>. level) image after multi-wavelet transform, (i) reconstructed image after 2<sup>nd</sup>. level multi-wavelet transform, (j) LL sub-band image after 2<sup>nd</sup>. level multi-wavelet transform, (k) (3<sup>rd</sup>. level) image after tensor product mixed transform, and (l) reconstructed image after tensor product mixed transform

Image quality is utilized to evaluate the achievement of the processed image [13]. The results are the average values of a set of many images used in the compression and quality metrics computation. Tables 1 and 2 show the 3-level compression and quality metrics computation values of WWT and MMT techniques. From the results shown in a 1<sup>st</sup> level technique comparative, M is the best technique because it has higher values of CR=16 and PSNR=54.6225. Also, it has the lowest values of MSE =0.2398, MD=1.0033, NAE=0.967, and SC=0.0305 than the W technique. Similarly, the PSNR is the most extensively used metric for the computation of reconstruction quality. A higher value of the PSNR specifies the reconstruction of the higher quality. Also, on the 2<sup>nd</sup>. and 3<sup>rd</sup>. levels comparative, the MMT is the best technique according to the compression and quality metrics values compared to the WWT technique.

Table 1. Compression and quality metrics computation values of WWT technique

WWT	CR	MSE	R(D)	PSNR	AD	MD	NAE	SC
1 <sup>st</sup> .level (W)	4	0.4687	4.4571	53.531	0.2195	1.0033	1.0869	0.9996
2 <sup>nd</sup> .level (W)	16	0.3082	3.41	53.538	0.1097	1.9947	0.8736	0.9983
3 <sup>rd</sup> .level (T)	64	0.4944	4.8643	51.46	0.1091	60.984	1.0276	0.9766

Table 2. Compression and quality metrics computation values of MMT technique

MMT	CR	MSE	R(D)	PSNR	AD	MD	NAE	SC
1 <sup>st</sup> .level (M)	16	0.2398	8.98	54.6225	0.3724	1.0033	0.967	0.0305
2 <sup>nd</sup> .level (M)	256	0.0072	1.24	69.7802	0.0183	0.466	0.9665	0.02994
3 <sup>rd</sup> .level (T)	1024	0.0003	4.154	81.9085	0.0007	2.0085	1.0482	0.9424

Table 3 presents the hybrid technique's compression, quality metrics and computation time (T):

$$T = \frac{2}{3}(1 - 4^{-L})N^2 \tag{10}$$

where L is the level's number, and N<sup>2</sup> is the image's size [18]. As shown from the results in a one-level comparison, the M technique is the best because it has higher values of CR=16 and PSNR=54.6225. Also, it

has the lowest values of MD, NAE, SC, and T. In the 2-level and 3-level techniques comparison, the MT and MMT techniques have efficient compression and quality metrics values among the other techniques.

**Table 3. Compression and quality metrics computation with T of the hybrid technique**

Technique/av.	CR	MSE	R(D)	PSNR	AD	MD	NAE	SC	T/sec.
W	4	0.4687	4.46	53.5303	0.2195	1.0033	1.0869	0.9996	0.1720
M	16	0.2398	8.978	54.6225	0.4199	1.0033	0.967	0.0305	0.0430
T	4	0.4997	28.48	51.4114	0.4384	59.6296	1.0139	0.9971	0.1720
WT	16	0.4979	13.769	52.2335	0.2188	60.0784	1.0200	0.9930	0.0430
MT	64	0.015	6.373	66.6034	0.019	10.6466	1.0277	0.9862	0.0108
WWT	64	0.4944	4.8643	51.46	0.1091	60.984	1.0276	0.9766	0.0108
WMT	256	0.0148	4.1755	66.6636	0.0094	10.9557	1.0368	0.9761	0.0027
MWT	256	0.0149	4.2266	66.6611	0.0094	10.9734	1.037	0.9761	0.0027
MMT	1024	0.0003	4.154	81.9085	0.0007	2.0085	1.0482	0.9424	6.7e-04

So, the M, MT, and MMT techniques have more significance in image compression and quality assessment applications because they have high performance and greater accuracy. Table 4 shows many distinct differences between a 2-level WW and MM in the previous work in [8] and the proposed techniques in a 2-level WW and MM in WWT and MMT techniques, respectively. In a WW, the CR<sub>prop.</sub>=16, the same as CR [8] but PSNR<sub>prop.</sub>=53.538, which is nearly twice the PSNR [8]. In the MM technique, the CR<sub>prop.</sub> is 16 times the CR [8] and the PSNR<sub>prop.</sub> is more significant than triple times the PSNR [8].

**Table 4. CR and PSNR of a 2-level comparison**

2-level comparison	CR <sub>prop.</sub>	PSNR <sub>prop.</sub>	CR [8]	PSNR [8]
WW	16	53.538	16	27.6408
MM	256	69.7802	16	28.1228

Table 5 shows a 3-level comparison between the proposed techniques and those used in 2017 [18] according to CR, R(D) and T. Although the proposed scheme WWT faces significant challenges, it successfully reduces the R(D) from 11.6792 in WWW [18] to 4.8643, with CR=64 still the same in the two techniques. The computation time (T) in WWW [18] is less than in WWT. Also, WWT reduces R(D) from 7.3689 in WWM [18] to 4.8643, but CR [18] reduced by a factor of 16, and T increased from 0.0025 to 0.0107. Finally, as compared, the WWT and MMT have values of R(D) less than values in WMW [18] and MMW [18] with the same CR=256 and 1024, respectively. While T is the same in MMW [18] and MMT, WMW [18] is faster than WMT by 0.1msec. The Letter S in WWS, MMS, and WMS refer to the stationary wavelet transform. The techniques WWT [18], MMT [18], and WMT [18] have the values of CR, R(D), and T better than that in the (WWS) [18], MMS [18], and WMS [18]. It is concluded that the results of the 2-level and 3-level proposed techniques have reliable quality.

**Table 5. CR, R(D) and T of a 3-level comparison**

3-level comparison	CR	R(D)	T/sec.
WWT	64	4.8643	0.0107
MMT	1024	4.154	0.0006
WMT	256	4.1755	0.0026
WWW [18]	64	11.6792	0.0102
WMW [18]	256	7.3927	0.0025
WWM [18]	256	7.3689	0.0025
MMW [18]	1024	4.5744	0.0006
WWS [18]	16	18.9526	0.041
MMS [18]	256	7.7415	0.0025
WMS [18]	64	12.2132	0.0102

#### 4. CONCLUSION

This paper evaluates the implementation of the hybrid techniques-based tensor product mixed transform. Compression and quality metrics computation are utilized for evaluating the hybrid techniques. The main contribution is to improve the hybrid techniques. The hybrid techniques consist of W, M, T, WT, MT, WWT, WMT, MWT, and MMT techniques. Compression and quality metrics are computed for the final levels,



and a comparison between techniques is implemented according to these metrics. The simulation results indicated that the M, MT, and MMT techniques have efficient compression and quality metrics. The MMT is the best among these three techniques, with  $CR=1024$ ,  $R(D)=4.154$ , and  $PSNR=81.9085$ . Also, it is faster than the other techniques in the previous works as compared with them. It can compress the image efficiently with high quality. Compared to the other methods, the improved compression and quality metrics justify the development and improvement in quantitative simulation results. There are no shortcomings in the proposed method. The conclusion of this study suggests that the research in this field could be directed to use a color or fingerprint image with the hybrid technique. Also, one can use a hybrid technique for image and speech recognition.




## REFERENCES

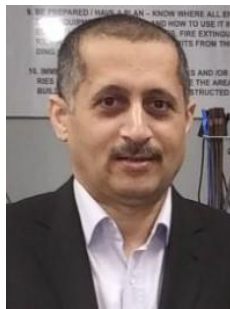
- [1] S. A. Mohammed, Z. Ibraheem, and A. A. Jassim, "Mixed transforms generated by tensor product and applied in data processing," *International Journal of Computer Applications*, vol. 81, no. 19, pp. 29–38, Nov. 2013, doi: 10.5120/14273-2351.
- [2] Z. Ibraheem, S. A. Mohammed, N. Jameel, and A. A. Jassim, "Performance study for mixed transforms generated by tensor product in image compression and processing," *Association of Arab Universities Journal of Engineering Sciences*, vol. 25, no. 3, pp. 155–168, 2018.
- [3] R. Kumar, U. Patbhaje, and A. Kumar, "An efficient technique for image compression and quality retrieval using matrix completion," *Journal of King Saud University - Computer and Information Sciences*, vol. 34, no. 4, pp. 1231–1239, Apr. 2022, doi: 10.1016/j.jksuci.2019.08.002.
- [4] A. Bouida, M. Beladgham, A. Bassou, and I. Benyahia, "Quality and texture analysis of biometric images compressed with second-generation wavelet transforms and SPIHT-Z encoder," *Indonesian Journal of Electrical Engineering and Computer Science (IJECS)*, vol. 19, no. 3, pp. 1325–1339, 2020, doi: 10.11591/ijeecs.v19.i3.pp1325-1339.
- [5] A. J. Qasim, R. Din, and F. Q. A. Alyousuf, "Review on techniques and file formats of image compression," *Bulletin of Electrical Engineering and Informatics (BEEI)*, vol. 9, no. 2, pp. 602–610, Apr. 2020, doi: 10.11591/eei.v9i2.2085.
- [6] S. Hu, L. Jin, H. Wang, Y. Zhang, S. Kwong, and C. C. J. Kuo, "Compressed image quality metric based on perceptually weighted distortion," *IEEE Transactions on Image Processing*, vol. 24, no. 12, pp. 5594–5608, Dec. 2015, doi: 10.1109/TIP.2015.2481319.
- [7] S. Abdul-wahed, M. Kamil, and H. A. Ahmed, "Compression of image using multi-wavelet techniques," *International Journal of Nonlinear Analysis and Applications*, vol. 13, no. 1, pp. 1519–1535, 2022, doi: 10.22075/IJNAA.2022.5768.
- [8] Z. I. Abood, "Image compression using 3-D two-level techniques," *Journal of Engineering*, vol. 19, no. 11, pp. 1407–1424, 2013.
- [9] A. O. Salau, S. Jain, and J. N. Eneh, "A review of various image fusion types and transforms," *Indonesian Journal of Electrical Engineering and Computer Science (IJECS)*, vol. 24, no. 3, p. 1515, Dec. 2021, doi: 10.11591/ijeecs.v24.i3.pp1515-1522.
- [10] U. Sara, M. Akter, and M. S. Uddin, "Image quality assessment through FSIM, SSIM, MSE and PSNR—a comparative study," *Journal of Computer and Communications*, vol. 07, no. 03, pp. 8–18, 2019, doi: 10.4236/jcc.2019.73002.
- [11] S. Athar and Z. Wang, "A comprehensive performance evaluation of image quality assessment algorithms," *IEEE Access*, vol. 7, pp. 140030–140070, 2019, doi: 10.1109/ACCESS.2019.2943319.
- [12] H. PhiCong, S. Perry, E. Cheng, and X. HoangVan, "Objective quality assessment metrics for light field image based on textural features," *Electronics*, vol. 11, no. 5, Mar. 2022, doi: 10.3390/electronics11050759.
- [13] F. Memon, M. A. Unar, and M. Sheeraz, "Image quality assessment for performance evaluation of focus measure operators," *Mehran University Research Journal of Engineering & Technology*, vol. 34, no. 4, pp. 389–386, 2015.
- [14] S. Hamida, O. E. Gannour, B. Cherradi, H. Ouajji, and A. Raihani, "Efficient feature descriptor selection for improved Arabic handwritten words recognition," *International Journal of Electrical and Computer Engineering (IJECE)*, vol. 12, no. 5, p. 5304, Oct. 2022, doi: 10.11591/ijece.v12i5.pp5304-5312.
- [15] S. K. Seetharamaswamy and S. K. Veeranna, "Super resolution image reconstruction via dual dictionary learning in sparse environment," *International Journal of Electrical and Computer Engineering (IJECE)*, vol. 12, no. 5, pp. 4970–4977, Oct. 2022, doi: 10.11591/ijece.v12i5.pp4970-4977.
- [16] H. A. Saeed, S. Hamad, and A. T. Hussain, "Analysis the digital images by using morphology operators," *Indonesian Journal of Electrical Engineering and Computer Science (IJECS)*, vol. 24, no. 3, p. 1654, Dec. 2021, doi: 10.11591/ijeecs.v24.i3.pp1654-1662.
- [17] I. Patel, S. Patel, and A. Patel, "Analysis of various image preprocessing techniques for denoising of flower images," *International Journal of Computer Sciences and Engineering*, vol. 6, no. 5, pp. 1111–1117, May 2018, doi: 10.26438/ijcse/v6i5.11111117.
- [18] Z. I. Abood, "Composite techniques-based color image compression," *Journal of Engineering*, vol. 23, no. 3, pp. 80–93, 2017.
- [19] S. S. Sann, S. S. Win, and Z. M. Thant, "An analysis of various image pre-processing techniques in butterfly image," *International Journal for Advance Research and Development*, vol. 6, no. 1, pp. 1–4, 2021.
- [20] W. A. Mahmoud, "Computation of wavelet and multiwavelet transforms using fast fourier transform," *Journal Port Science Research*, vol. 4, no. 2, pp. 102–108, Dec. 2021, doi: 10.36371/port.2020.2.7.
- [21] T. S. Aina, O. Akinte, B. Ademola, and A. Iriaoghuan, "Wavelet transforms and image approximation based image compression system," *International Journal of Scientific & Technology Research*, vol. 10, no. 10, pp. 104–107, 2021.
- [22] L. Fan, "Retracted article: Image processing algorithm of Hartmann method aberration automatic measurement system with tensor product model," *EURASIP Journal on Image and Video Processing*, vol. 2019, no. 1, p. 43, Feb. 2019, doi: 10.1186/s13640-019-0440-9.
- [23] M. Jallouli, M. Zemni, A. B. Mabrouk, and M. A. Mahjoub, "Toward new multi-wavelets: associated filters and algorithms. Part I: theoretical framework and investigation of biomedical signals, ECG, and coronavirus cases," *Soft Computing*, vol. 25, no. 22, pp. 14059–14079, Nov. 2021, doi: 10.1007/s00500-021-06217-y.
- [24] Y. Panagakis *et al.*, "Tensor methods in computer vision and deep learning," *Proceedings of the IEEE*, vol. 109, no. 5, pp. 863–890, May 2021, doi: 10.1109/JPROC.2021.3074329.
- [25] A. Cazañas-Gordón and E. Parra-Mora, "Digital compression in medical images compresión digital en imágenes médicas," *Latin-American Journal of Computing*, vol. 9, no. 1, pp. 60–70, 2022, doi: 10.5281/zenodo.5816321.
- [26] D. Y. Abbaas, "Fractal image compression based on high entropy values technique," *Al-Mustansiriyah Journal of Science*, vol. 28, no. 2, pp. 119–133, Apr. 2018, doi: 10.23851/mjs.v28i2.507.




- [27] G. Zacharis, G. Gadounas, P. Tsirtsakis, G. Maraslidis, N. Assimopoulos, and G. Fragulis, "Implementation and optimization of image processing algorithm using machine learning and image compression," *SHS Web of Conferences*, vol. 139, p. 03014, May 2022, doi: 10.1051/shsconf/202213903014.
- [28] H. A. Alasadi, "Image compression algorithms based on discrete multi-wavelet transform," *Kufa Journal of Engineering*, vol. 8, no. 3, pp. 119–127, 2017.
- [29] A. S. Abd-Alzhra and M. S. H. Al-Tamimi, "Image compression using deep learning: methods and techniques," *Iraqi Journal of Science*, vol. 63, no. 3, pp. 1299–1312, Mar. 2022, doi: 10.24996/ij.s.2022.63.3.34.
- [30] M. Kawawa-Beaudan, R. Roggenkemper, and A. Zakhor, "Recognition-aware learned image compression," *Electronic Imaging*, vol. 34, no. 14, pp. 220-1-220-5, Jan. 2022, doi: 10.2352/EI.2022.34.14.COIMG-220.
- [31] S. I. Abood, *Continuous and Discrete Signals*. CRC Press, 2020.
- [32] A. H. Shini, Z. I. Abood, and T. Z. Ismaeel, "Hybrid techniques-based speech recognition," *International Journal of Computer Applications*, vol. 139, no. 10, pp. 12–18, 2016.
- [33] A. Rubel, O. Ieremeiev, V. Lukin, J. Fastowicz, and K. Okarma, "Combined no-reference image quality metrics for visual quality assessment optimized for remote sensing images," *Applied Sciences*, vol. 12, no. 4, p. 1986, Feb. 2022, doi: 10.3390/app12041986.
- [34] R. Kazmierczak, G. Franchi, N. Belkhir, A. Manzanera, and D. Filliat, "A study of deep perceptual metrics for image quality assessment," *arXiv preprints*, Feb. 2022, [Online]. Available: <http://arxiv.org/abs/2202.08692>.
- [35] S. M. H. Mousavi and S. M. H. Mosavi, "A new edge and pixel-based image quality assessment metric for colour and depth images," in *2022 9th Iranian Joint Congress on Fuzzy and Intelligent Systems (CFIS)*, Mar. 2022, pp. 1–11, doi: 10.1109/CFIS54774.2022.9756490.
- [36] M. W. Mirza, A. Siddiq, and I. R. Khan, "A comparative study of medical image enhancement algorithms and quality assessment metrics on COVID-19 CT images," *Signal, Image and Video Processing*, pp. 1–10, Apr. 2022, doi: 10.1007/s11760-022-02214-2.
- [37] S. Rajkumar and G. Malathi, "A comparative analysis on image quality assessment for real time satellite images," *Indian Journal of Science and Technology*, vol. 9, no. 34, Sep. 2016, doi: 10.17485/ijst/2016/v9i34/96766.

## BIOGRAPHIES OF AUTHORS






**Zainab Ibrahim Abood Al-Rifaae**    received her B.Sc. and M.Sc. degree in Electrical Engineering from College of Engineering, University of Baghdad, Iraq. She has been a faculty member since 2009 and is currently an Assistant Professor at the Department of Electrical Engineering, University of Baghdad, Iraq. Her research interest includes digital signal and image processing, communication, and information security. She can be contacted at email: [zainab.ibrahim@coeng.uobaghdad.edu.iq](mailto:zainab.ibrahim@coeng.uobaghdad.edu.iq).



**Samir Ibrahim Abood**    received his B.S. and M.S. from the University of Technology, Baghdad, Iraq, in 1996 and 2001; respectively, he got his Ph.D. in the Electrical and Computer Engineering Department at Prairie View A & M University. From 1997 to 2001, he worked as an engineer at the University of Technology. From 2001 to 2003, he was a professor at the University of Baghdad and Al-Nahrain University. From 2003 to 2016, Mr. Abood was a professor at Middle Technical University / Baghdad-Iraq. From 2018 to the present, he has worked at Prairie View A & M University/ Electrical and Computer Engineering Department. He is the author of 30 papers and ten books. His main research interests are sustainable power and energy systems, microgrids, power electronics and motor drives, digital PID controllers, digital methods for electrical measurements, digital signal processing, and control systems. He can be contacted at email: [siabood@pvamu.edu](mailto:siabood@pvamu.edu).



**Prof. Dr. Tarik Zeyad Ismaeel**    has been a faculty member at a University of Baghdad, College of Engineering, Electrical Engineering Department since 1994. His research interest includes communication, information security, digital signal and image processing. He can be contacted at email: [tarik.z@coeng.uobaghdad.edu.iq](mailto:tarik.z@coeng.uobaghdad.edu.iq).